

Heterogeneous Relationships of Subjects and Shapelets for Semi-supervised Multivariate Series Classification

Mingsen Du^a, Yongjian Li^a, Meng Chen^a, Cun Ji^{b,*}, Shoushui Wei^{a,*}

^a School of Control Science and Engineering, Shandong University, Jinan, China

^b School of Information Science and Engineering, Shandong Normal University, Jinan, China

mingsendu@mail.sdu.edu.cn, lyj4072021@163.com, chchenmeng@gmail.com, jicun@sdu.edu.cn, sswei@sdu.edu.cn

Abstract—Multivariate time series (MTS) classification is widely applied in fields such as industry, healthcare, and finance, aiming to extract key features from complex time series data for accurate decision-making and prediction. However, existing methods for MTS often struggle due to the challenges of effectively modeling high-dimensional data and the lack of labeled data, resulting in poor classification performance. To address this issue, we propose a heterogeneous relationships of subjects and shapelets method for semi-supervised MTS classification. This method offers a novel perspective by integrating various types of additional information while capturing the relationships between them. Specifically, we first utilize a contrast temporal self-attention module to obtain sparse MTS representations, and then model the similarities between these representations using soft dynamic time warping to construct a similarity graph. Secondly, we learn the shapelets for different subject types, incorporating both the subject features and their shapelets as additional information to further refine the similarity graph, ultimately generating a heterogeneous graph. Finally, we use a dual level graph attention network to get prediction. Through this method, we successfully transform dataset into a heterogeneous graph, integrating multiple additional information and achieving precise semi-supervised node classification. Experiments on the Human Activity Recognition, sleep stage classification and University of East Anglia datasets demonstrate that our method outperforms current state-of-the-art methods in MTS classification tasks, validating its superiority.

Index Terms—Heterogeneous Graph, Multivariate Time Series Classification, Representation Learning, Shapelets, Graph Attention Network

I. INTRODUCTION

Multivariate time series (MTS) classification is of significant importance in many practical applications, especially in fields such as industrial control [1], healthcare monitoring [2], financial market analysis [3], and human activity recognition (HAR) [4].

However, in many practical situations, labeled data is scarce, and the manual labeling process is time-consuming and often requires expert knowledge. Supervised models are typically optimized for data from specific tasks or domains, which

can lead to poor generalization when faced with new tasks or different data distributions. Additionally, label noise or annotation errors can directly affect model performance; in the case of MTS, inaccurate labels may hinder the model's ability to effectively capture complex temporal relationships. Therefore, there is an urgent need to investigate methods that can effectively perform MTS classification with limited labeled data.

Unsupervised [5], [6] or self-supervised [7], [8] representation learning eliminates the need for extensive labeled data and can fully utilize unlabeled data for temporal representation learning, thereby enhancing the model's generalization ability and applicability. Such methods can extract underlying structures and patterns. Compared to supervised learning, these methods generally possess stronger generalization capabilities because they learn more universal feature representations rather than those targeted at specific tasks or labels. Additionally, these approaches are less sensitive to label noise and can adaptively improve the model's representation learning ability as the data volume increases, making them more robust when dealing with noise and incomplete data. Moreover, existing methods for MTS still face the following challenges.

Firstly, MTS are typically generated by multiple sensors, each capturing different types of features, making their high dimensionality a challenge for time series representation learning [9], among which Transformer [10] shines in representation learning. Currently, most Transformer-based methods often embed all channels into a fixed-length vector and use self-attention mechanisms to capture the correlations between time points. However, this approach has several obvious issues. First, embedding all channels into a unified representation neglects the independence among channels. Next, computing self-attention for time point tends to make the model focus more on global information, overlooking local feature variations. Moreover, as the sequence length increases, the computational complexity of Transformers grows quadratically, resulting in low computational efficiency.

In contrast, calculating features for each channel separately and treating the sliding window as a token can better capture the temporal dynamics of each channel while preserving the independence among channels. By treating the sliding window as a token, the model can focus on changes and patterns within

This work was supported by the National Natural Science Foundation of China [grant numbers 82072014], the National Key R&D Program of China [grant numbers 2019YFE010670], the Shandong Province Natural Science Foundation [grant numbers ZR2020MF028].

*Corresponding author: Shoushui Wei (sswei@sdu.edu.cn), Cun Ji (jicun@sdu.edu.cn).

specific time periods, aligning better with the importance of local features in real-world scenarios. Additionally, this method offers higher sparsity by calculating attention on local tokens, improving overall computational efficiency.

Secondly, the correlation between dimensions in MTS is an essential feature, leading to the emergence of numerous graph modeling methods based on graph neural networks (GNN) [11]. Current research on graph modeling methods using GNN typically focuses on modeling relationships between dimensions [12]. In recent years, GNN-based graph modeling approaches have gained widespread attention and have been applied to capture relationships between dimensions. Current studies employ GNN to model the homogeneous or heterogeneous [13], [14] relationships between MTS dimensions. In homogeneous graph modeling, different dimensions are treated as nodes of the same type, with the focus on capturing similarities or correlations between dimensions and extracting global features through a shared graph structure. Methods for handling heterogeneous networks [15]–[17] requires consideration of structural information composed of various types of nodes and edges. The heterogeneity and rich semantic information present significant challenges in designing heterogeneous graph neural networks.

Finally, methods lack interpretability. Shapelets [18]–[20] are interpretable local subsequences that can maximally represent a class of samples and reflect the basis of classification decisions, making it easier for experts to understand their significance. However, in MTS classification, due to subject differences, time series of the same category may exhibit different shapes of shapelets. When dealing with data involving subject differences, capturing more targeted feature variations becomes particularly important. For instance, in HAR tasks, data may come from populations of different ages. Biomedical signals often originate from the physiological characteristics of different patients. These subject differences can lead to variations in time series patterns or shapelets.

By generating personalized subject shapelets [21], models can more accurately capture the unique time series patterns of each subject or category, rather than only relying on general global features. The extraction of personalized shapelets allows the model to effectively distinguish features between different subjects, thereby enhancing the robustness and interpretability ability of classification.

Therefore, to solve the above problems, we propose heterogeneous relationships of subjects and shapelets method with heterogeneous graph representation learning (HGRL) for semi-supervised MTS classification, which can integrate subject features and shapelet information as supplementary information while capturing the relationships between them. Specifically, we first obtain sparse representations of MTS through a contrast temporal self-attention module, which adopts a new positive and negative data sampling strategy with the contrast temporal representation loss to obtain the MTS representation. Then, we use soft DTW to model the similarity between MTS representations, constructing a representation graph. Next, we learn the exclusive shapelets for the subjects. To achieve

this, we incorporate subject features and the corresponding shapelets as additional information in the representation graph, resulting in the final heterogeneous graph. Finally, dual GAT introduce node-level attention to learn the importance between nodes, and type-level attention to manage the relationships between different types of information (such as shapelet features, subject features, and MTS representation features), ensuring the effective integration and expression of multi-type information. Our contributions are as follows:

- 1) To the best of our knowledge, we are the first to represent MTS dataset as heterogeneous graph and integrate subject features and shapelet information for MTS node classification.
- 2) We develop a contrast temporal self-attention, which picks principal dimensions in the sample and uses contrast temporal loss for MTS representations learning.
- 3) We make our method interpretable by learning multi-scale shapelets with subject differences.
- 4) We propose a heterogeneous graph representation learning method, and conducted experiments on multiple MTS datasets to validate the superiority.

II. RELATED WORK

A. Graph based methods

Recently, some GNN-based methods graph classification and node classification have been proposed. For graph classification, we introduce it from the aspects of homogeneous graph, heterogeneous graph.

For homogeneous graph, Time2Graph++ [22] addresses this by introducing a time-level attention mechanism to extract time-aware shapelets. Subsequently, time series data is transformed into shapelet evolution graphs to capture evolving patterns, further enhanced by graph attention to improve shapelet evolution. TS-GAC [23] introduces graph augmentation techniques for nodes and edges to maintain the stability of sensors and their associations. Subsequently, robust sensor and global features are extracted through node- and graph-level contrast.

For heterogeneous graph, SleepHGNN [15] captures both the interactivity and heterogeneity of physiological signals through its heterogeneous graph transformer layers. These layers consist of a heterogeneous message passing module to handle signal heterogeneity and a target-specific aggregation module to model signal interactivity. MTHetGNN [13] features a relation embedding module to represent complex relationships among variables as graph nodes and edges, along with a temporal embedding module for feature extraction. The model integrates these components to capture both static and dynamic dependencies.

Another application of GNN is node classification [24], where each sample in the data set is regarded as a node. Recently, several research [25] treats time series as nodes in a graph, with node similarity calculated using DTW and incorporated into the GNN. Due to the high complexity of DTW, further research [26] uses the lower bound of DTW to calculate similarity, reducing the time complexity.

B. Representation learning based methods

MTS representation mainly consists of time series representation and its graph representation. TS-TCC [8] creates two correlated views of time-series data through weak and strong augmentations. It uses a temporal contrasting module for robust representation learning via cross-view prediction. And it uses a contextual contrasting module to enhance discrimination by maximizing similarity within a sample and minimizing it across samples. AVGNets [27] reconstructs weighted graphs using angular visibility to retain both sequential and structural information in time series, addressing information loss in traditional visibility graph encodings. It features a ProbAttention module to extract temporal dependencies across multi-layer graphs, enhancing representation learning and improving forecasting performance.

C. Semi-supervised methods

In recent years, a large number of semi-supervised methods have been proposed. SSL [28] enhances semi-supervised learning by leveraging both time-domain and frequency-domain views through temporal-frequency co-training. It trains two deep neural networks simultaneously, using pseudo-labels from one view to guide the other, and incorporates a supervised contrastive learning module to improve representation quality. SSML [29] presents a semi-supervised meta-learning framework combined with adversarial training to tackle multi-source heterogeneity in time series data, focusing on heterogeneous features and labeling uncertainty. DiffShape [30] utilizes a semi-supervised and self-supervised diffusion learning mechanism that conditions on real subsequences, enhancing the similarity between learned shapelets and actual subsequences using abundant unlabeled data. It also employs a contrastive language-shapelets strategy, integrating natural language descriptions to improve the discriminability of learned shapelets.

III. METHOD

A. Overview

Previous research has typically enriched time series representations by extracting various features and methods. However, these approaches often overlook additional information, such as subject differences (e.g. variations in data collect timestamps). In contrast, our method integrates such extra information and models the complex relationships between these factors and the time series.

- 1) Specifically, firstly, we use a contrast temporal self-attention (CTSA) module to obtain sparse representations, and soft DTW to model similarity graph representation (Section III-B).
- 2) Secondly, we learn subject shapelets for each subject type in the dataset. To do this, we utilize a multi-task loss that includes both subject label loss and sample label loss (Section III-C).
- 3) Thirdly, we use T5 [33] model to embed subject information as subject features, without affecting the training weights (Section III-E).

- 4) Consequently, we add subject features and shapelets as additional information for the similarity graph, forming a heterogeneous graph (Section III-F).
- 5) Finally, we apply a dual level GAT to aggregate information from heterogeneous graph. It includes node-level attention, which learns the importance of nodes and effectively identifies the most influential samples, and type-level attention, which captures relationships between different types (shapelets, subject features and MTS representations) (Section III-G).

A simple heterogeneous graph node classification is shown in Fig. 1. The intuitive process is shown in Algorithm 1.

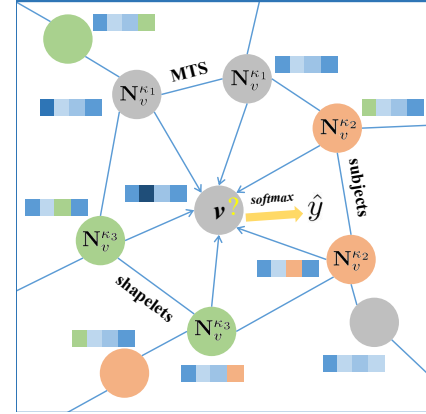


Fig. 1: A brief diagram of heterogeneous graph node classification

B. Similarity Graph Representation Learning

We use a CTSA module with contrast temporal loss to obtain MTS sparse representations (Section III-B1). Then, we apply the soft DTW loss to model the similarity between these representations, thus obtaining similarity graph representation (Section III-B2).

1) *CTSA*: Current self-attention-based methods directly embed all channels into fixed-length vectors and obtain correlations by calculating self-attention between time points. While it treats the entire time series as a whole, making it ineffective in capturing local patterns, while the dense computations of the self-attention mechanism result in extremely high computational costs.

To solve above problems, we introduce temporal self-attention module. Then, to obtain MTS representations, we introduce contrast temporal loss, allowing the model to learn features based on the similarity between anchor, positive, and negative samples without relying on labels, making it well-suited for self-supervised learning. By combining the sliding window method with contrast temporal loss, we can enhance the model's sensitivity to local features and variations within the MTS while maintaining computational efficiency. The overview structure of CTSA is shown in Fig. 2.

Temporal Self-Attention: We use sliding window to partition MTS into overlapped segments (i.e., tokens) and calculate the attention between these tokens as the following steps.

Algorithm 1 The process of the HGRL

- 1: **Input:** MTS dataset \mathcal{D}
 - 2: **Output:** Predict label \hat{y}
 - 3: **for** each MTS T from \mathcal{D} **do** \triangleright **Step 1:** Obtain similarity graph representations D
 - 4: $T_{ref}, T_{pos}, T_{neg} \leftarrow T$ \triangleright Creat anchor, positive, negative sample
 - 5: $T_{rep} \leftarrow \text{CTSA}(T_{ref}, T_{pos}, T_{neg})$ \triangleright Use CTSA module to get MTS Representations
 - 6: Update \mathcal{L}_{rep}
 - 7: **end for**
 - 8: **for** $i = 1$ to n **do**
 - 9: **for** $j = i + 1$ to n **do**
 - 10: $d_{i,j} \leftarrow \text{SoftDTW}(T_{rep}^i, T_{rep}^j)$ \triangleright Compute DTW similarity between MTS Representations
 - 11: $D[j, i] \leftarrow D[i, j] \leftarrow d_{i,j}$ \triangleright It is symmetric
 - 12: **end for**
 - 13: **end for**
 - 14: **for** each epoch e in \mathcal{E} **do** \triangleright **Step 2:** Learn subject shapelets s
 - 15: $s \leftarrow \text{LearnShapelets}(D)$ \triangleright Learn Shapelets
 - 16: $\mathcal{L}_s \leftarrow \mathcal{L}_{sub} + \mathcal{L}_{sam}$
 - 17: Update \mathcal{L}_s \triangleright Compute multi-task loss
 - 18: **end for**
 - 19: $F_{sub} \leftarrow \text{T5}(sub)$ \triangleright **Step 3:** Get subject label embedding F_{sub} using T5 model
 - 20: $\tilde{\mathcal{A}} = \text{relation}(\text{MTS}, \text{subject}, \text{shapelets})$ \triangleright **Step 4:** Get relationships between MTS, subjects, shapelets to form a heterogeneous graph
 - 21: **for** each epoch e in \mathcal{E} **do** \triangleright **Step 5:** Heterogeneous graph representation learning using dual level GAT
 - 22: $\hat{y} \leftarrow \text{dualGAT}((\mathcal{A}, T_{rep}, s, F_{sub}), \mathcal{B})$ \triangleright Predict label
 - 23: update parameters \mathcal{B}
 - 24: **end for**
-

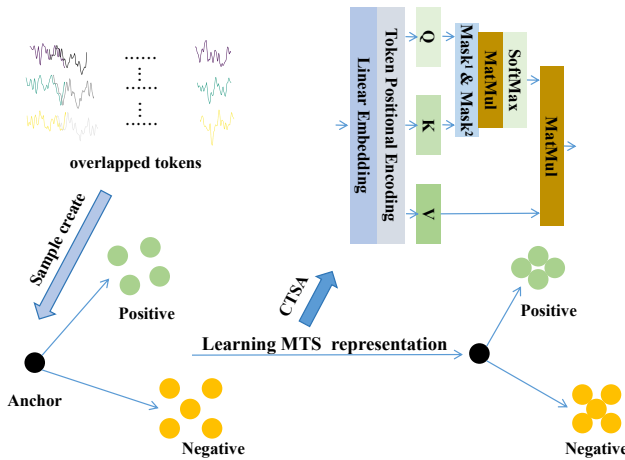


Fig. 2: Overview of CTSA module

First, the sliding window is treated as a token to capture attention between tokens, as it is meaningful to study the characteristics or changes of time series over a specific period. We apply a mask matrix to ensure that attention calculations are performed only within the same dimension. Additionally, we designed another mask matrix to prevent self-attention computation when there is a large overlap in the tokens of the current dimension. Overlapping subsequences often contain repeated information, and calculating the self-attention between them may lead to redundancy. Therefore, not calculating the attention of subsequences that overlap too much can make the model more focused on capturing unique features and changes, improving learning efficiency. This sliding window method ensures that attention can focus on meaningful local features and changes within each dimension, allowing for better capture of the local characteristics of each time series. Furthermore, by calculating attention separately for each dimension and leveraging the sparsity of the generated attention matrix, we can significantly reduce computational overhead and improve model efficiency.

Let the time series $T \in \mathbb{R}^{C \times L}$, where C is the number of channels and L is the length of the time series. And each token has a length of W and is sampled at intervals of S . Then, each dimension is segmented into tokens with window length W , sliding step S as tokens = $\{T[i : i + W] \mid i = 0, S, 2S, \dots, L - W\}$. After getting tokens T_{to} , we compute the self-attention between tokens. For tokens T_t , we calculate query, key, and value as (1), where W^Q is query weight, W^K is key weight, W^V is value weight.

$$Q_{to} = W^Q T_{to}, \quad K_{to} = W^K T_{to}, \quad V_{to} = W^V T_{to} \quad (1)$$

The attention weight A_t is calculated a (2) combining the masking matrices to calculate sparse weighted attention. In (2), M_1 ensures that attention calculations are performed only within the same dimension as (3). M_2 prevent self-attention computation when there is a large overlap ratio γ_1 in the tokens of the current dimension as (4). \mathbb{I} represents the indicator function, which returns value of 1 indicates that the condition is met, and returns value of 0 indicates that the condition is not met.

$$A_t = \text{softmax} \left(\frac{Q_{to}^T K_{to}}{\sqrt{d_k}} \right) \cdot M_1 \cdot M_2 \cdot V_{to} \quad (2)$$

$$M_1^{i,j} = \mathbb{I} \left(\text{dim}(T_{to}^i) = \text{dim}(T_{to}^j) \right) \quad (3)$$

$$M_2^{i,j} = \mathbb{I} \left(\text{overlap}(T_{to}^i, T_{to}^j) < \gamma_1 \right) \quad (4)$$

Contrast Temporal Loss: Specifically, the anchor is drawn from continuous overlapping subsequences in certain dimensions, while the positive sample is from the same dimension and overlaps with the anchor. The negative sample is selected from subsequences in different dimensions that show significant feature differences from the anchor.

The overlap between the anchor and the positive sample enables the model to capture subtle variations within the same dimension, thereby improving the learning of local features.

Meanwhile, the introduction of negative samples encourages the model to focus on distinguishing features across different dimensions during training. By selecting negative samples from different dimensions, the model effectively reduces its sensitivity to noise and interference, improving its generalization ability when handling complex time series data. We borrowed the idea of triplet loss [31], which aims to minimize the distance between the anchor and the positive sample while maximizing the distance between the anchor and the negative sample. This optimization helps form clearer decision boundaries in the feature space, leading to more accurate similarity comparisons.

However, there is still a question: how to choose the dimension to keep the most features of MTS. To do this, we select principal component dimensions instead of random dimensions. Principal component analysis identifies the dimensions that capture the most variance. These dimensions are more likely to hold meaningful patterns, making them more informative for downstream tasks. Using principal components ensures that selected features are those that most effectively represent the data’s underlying structure.

We find the principal dimensions by followings.

First, we perform data centering by $T_{\text{centered}} = T - \mu$. Next, we compute the covariance matrix M_C of the centered time series by $M_C = \frac{1}{n-1} T_{\text{centered}}^T T_{\text{centered}}$. Here, n is the number of time points in the series.

Finally, we perform eigenvalue decomposition on the covariance matrix M_C to compute its eigenvalues λ_i and corresponding eigenvectors v_i using $M_C v_i = \lambda_i v_i$. The principal components correspond to the eigenvectors with the largest eigenvalues λ_i , and the dimensions associated with those eigenvectors are the principal component dimensions T_p . After

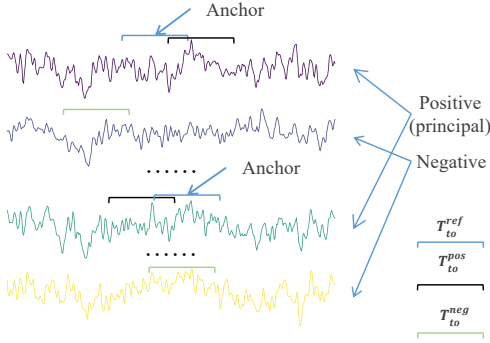


Fig. 3: Rules for selecting anchor, positive, negative samples

getting principals, we select positive and negative samples by the following criteria, as shown in Fig. 3.

Anchor Samples T_{to}^{ref} . The anchor point is chosen from the principal component dimensions. We select m dimensions from the principal components of the time series and obtain continuous tokens from these dimensions to serve as the anchor T_{ref} . For example, at time t_1 in dimension i , the anchor

can be defined as:

$$T_{to}^{\text{ref}} = T_{to}^{i,t_1} \oplus T_{to}^{i,t_1+S} \oplus \dots \oplus T_{to}^{i,t_1+(W-1)S} \quad (5)$$

Positive Samples T_{to}^{pos} . Select other tokens that are continuous and overlap with the anchor T_{ref} . The positive samples come from the same principal component dimension, but with an overlapping time range as the anchor T_{ref} . If the anchor covers the time range $[t_1, t_1 + W)$, positive samples can be selected as:

$$T_{to}^{\text{pos}} = T_{to}^{i,t_1+k} \oplus T_{to}^{i,t_1+k+S} \oplus \dots \oplus T_{to}^{i,t_1+k+(W-1)S} \quad (6)$$

where k can take values $0, S, 2S, \dots$ (as long as $t_1 + k + W$ does not exceed the length of the series).

Negative Samples T_{to}^{neg} . Negative samples are chosen from non-principal component dimensions. These are tokens that come from other dimensions, excluding those selected as principal components. Negative samples can be expressed as:

$$T_{to}^{\text{neg}} = T_{to}^{j,t_2} \oplus T_{to}^{j,t_2+S} \oplus \dots \oplus T_{to}^{j,t_2+(W-1)S} \quad (7)$$

where $j \neq i$, meaning they are from dimensions other than the anchor’s principal components.

After obtaining positive and negative samples, we obtain the MTS representations as (8). Where $f(\cdot, \theta)$ is embedding from CTSA module function with parameters θ . $\cos(f(T_{to}^{\text{ref}}, \theta), f(T_{to}^{\text{pos}}, \theta)) = f(T_{to}^{\text{ref}}, \theta) \cdot f(T_{to}^{\text{pos}}, \theta) / (\|f(T_{to}^{\text{ref}}, \theta)\| \|f(T_{to}^{\text{pos}}, \theta)\|)$. σ is the sigmoid function. K is the number of negative samples.

$$\mathcal{L}_{\text{rep}} = -\log(\sigma(\cos(f(T_{to}^{\text{ref}}, \theta), f(T_{to}^{\text{pos}}, \theta)))) - \sum_{k=1}^K \log(\sigma(-\cos(f(T_{to}^{\text{ref}}, \theta), f(T_{to}^{\text{neg}k}, \theta)))) \quad (8)$$

The triplet construction (anchor, positive and negative samples) and cosine similarity calculation can effectively learn discriminative MTS representations. This approach refines the embedding space, focusing on principal components and critical features, thereby enhancing the accuracy and reliability of subsequent similarity calculations.

2) *Similarity Graph Representation:* To align the temporal dynamics for a more accurate similarity of MTS representations, we note that when using DTW to calculate high-dimensional MTS, the dimensions are typically aggregated to compute an average. This approach, however, results in the loss of various key features inherent in each dimension. To address this issue, we employ the CTSA module to obtain a robust MTS representations T_i^{rep} . This enables us to use DTW to achieve a more efficient and effective similarity representation.

To tackle the challenge of non-minimizability in the DTW algorithm, [32] introduced the concept of soft minimum as a substitute for the DTW minimum. They designed the minimizable soft DTW loss function to model similarity through the following steps. The soft DTW loss function combines the smooth minimum operator with dynamic programming to compute a differentiable and robust measure of alignment

between time series, which can be used in optimization tasks such as training time series models.

We first compute the accumulated cost using the dynamic programming recursion as $r_{i,j} = \|T_i^{rep} - T_j^{rep}\|_2^2$. The cost matrix $r_{i,j}$ is defined as the squared Euclidean distance between the i -th element of time series T_i^{rep} and the j -th element of time series T_j^{rep} . Then, the dynamic programming matrix $D_{i,j}$ accumulates the costs for aligning subsequences of T_i^{rep} and T_j^{rep} , and is computed recursively as $D_{i,j} = r_{i,j} + \min_{\gamma_2} \{D_{i,j-1}, D_{i-1,j}, D_{i-1,j-1}\}$

Next, we compute the smooth minimum operator, as expressed in (9). The operator is defined with a smoothing parameter γ_2 , which determines how much smoothing is applied to the minimum operation. For $\gamma_2 > 0$, the operator computes a smoothed version of the minimum by applying a weighted sum of exponentials:

$$\min_{\gamma_2} \{a_1, \dots, a_n\} = \begin{cases} \min\{a_1, \dots, a_n\}, & \text{if } \gamma_2 = 0 \\ -\gamma_2 \log \left(\sum_{i=1}^n e^{-a_i/\gamma_2} \right), & \text{if } \gamma_2 > 0 \end{cases} \quad (9)$$

Finally, we define the soft DTW loss as (10), where $\text{DTW}_{\gamma_2}(T_i, T_j)$ is the soft DTW distance. The alignment matrix set $A_{n,m}$ consists of all possible binary alignment matrices of size $n \times m$, where each element A represents a specific alignment between the two sequences:

$$\text{DTW}_{\gamma_2}(T_i^{rep}, T_j^{rep}) = \min_{\gamma_2} \{ \langle A, \Delta(T_i^{rep}, T_j^{rep}) \rangle \mid A \in A_{n,m} \} \quad (10)$$

where $\langle A, \Delta(\cdot) \rangle$ is the inner product, which quantifies the alignment cost between T_i^{rep} and T_j^{rep} . $A_{n,m}$ represents the set of all possible binary matrices $A \in \{0, 1\}^{n \times m}$, where each matrix corresponds to a valid alignment of the two sequences. A specific matrix A has values of 1 for the points along the alignment path and 0 elsewhere.

After getting the DTW matrix: $\text{DTW}_{\gamma_2}(T_i^{rep}, T_j^{rep})=D$, to further describe the similarity, we perform the following processing. The similarity matrix D_{sim} is obtained by the following formula as (11) - (12).

We first compute the normalized distance between elements i and j as D_{ij}^{norm} .

$$D_{ij}^{\text{norm}} = (D_{ij} - D_{\min}) \cdot (D_{\max} - D_{\min})^{-1} \quad (11)$$

After normalization, the distance values are converted to similarity values using an exponential function with a scaling parameter α , which controls the rate of decay in similarity as distance increases.

The final similarity matrix D_{sim} is defined by 12. $\alpha \in [0, \infty)$ is a tuning parameter that controls the sensitivity of the similarity to distance values. Higher values of α make the similarity decay faster as the distance increases.

$$D_{sim} = \exp(\alpha \cdot D_{ij}^{\text{norm}})^{-1} + 1 \quad (12)$$

C. Subject Shapelets Learning

We introduce subject-specific shapelets in the heterogeneous graph framework, allowing the model to capture specific patterns of different subjects. This is particularly important for

applications such as HAR, industrial monitoring, or biomedical signal analysis, which often show subject differences due to factors such as age differences, operating conditions, or patient physiological characteristics.

We build a multi-task model using subject type as label and sample label for multi-scale shapelets learning. The model can learn features that distinguish different subject types and learning corresponding shapelets.

Shapelets learning is completed by the following two tasks. Sample shapelet learning: Get sample prediction probabilities \hat{y}_{sample} . Subject shapelet learning: Get subject prediction probabilities \hat{y}_{sub} . In detail, there are following steps:

For each scale s_k^ℓ (where ℓ represents the scale), we compute the Euclidean distance between the shapelet s_k^ℓ and subsequence T_ϕ^m of time series T_m as:

$$d(s_k^\ell, T_\phi^m) = \sqrt{\sum_{l=1}^{L^\ell} (s_l^{k,\ell} - x_{\phi+l-1}^m)^2} \quad (13)$$

where s_k^ℓ is the ℓ -th scaled shapelet. L^ℓ is the length of the shapelet at scale ℓ . $s_l^{k,\ell}$ is the l -th element of the shapelet s_k^ℓ . $x_{\phi+l-1}^m$ is the $(\phi + l - 1)$ -th element of the m -th time series.

Next, we compute the distance between the shapelet s_k^ℓ at scale ℓ and the entire time series T_j^m . The Soft-Minimum calculation is adapted for multi-scale shapelets:

$$D(s_k^\ell, T_j^m) = \text{SoftMini}(d_1^{m,k,\ell}, d_2^{m,k,\ell}, \dots, d_j^{m,k,\ell}) \quad (14)$$

where $d_\zeta^{k,m,\ell}$ is the distance between the ℓ -scaled shapelet and the ζ -th subsequence of the m -th time series at scale ℓ . The Soft-Minimum formula is computed as:

$$D(s_k^\ell, T_j^m) = \frac{\sum_{\zeta=1}^j d_\zeta^{k,m,\ell} e^{\delta_1 d_\zeta^{k,m,\ell}}}{\sum_{\zeta'=1}^j e^{\delta_1 d_{\zeta'}^{k,m,\ell}}} \quad (15)$$

where δ_1 is a scaling factor, and j is the number of subsequences in the time series.

Finally, the prediction, soft minimum loss, and total loss calculations are computed as follows:

$$\hat{y} = W_0^c + \sum_{k=1}^K D_{k,m}^j W_k^c \quad (16)$$

$$\mathcal{L}_{\text{sam}} = -\frac{1}{M} \sum_{m=1}^M \sum_{c=1}^C y_c^{m,j} \log(\hat{y}) \quad (17)$$

$$\mathcal{L}_s = \lambda \mathcal{L}_{\text{sam}} + (1 - \lambda) \mathcal{L}_{\text{sub}} \quad (18)$$

where $y_c^{m,j}$ is the true label for the m -th sample in class c . W_k^c is the weight for the k -th shapelet in the classifier for class c .

Further, to reduce redundancy among shapelets, we compare the similarity between shapelets at different scales. If two shapelets $s_k^{\ell_1}$ and $s_p^{\ell_2}$ are too similar, or if one shapelet is a subset of another, we discard one of them to reduce redundancy. The similarity between shapelets can be computed using their soft DTW distance $\text{DTW}(s_k^{\ell_1}, s_p^{\ell_2})$ as (10). If the

similarity between shapelets exceeds a threshold τ_{sim} , or if the shapelet at one scale is too close to another, the redundant shapelet $s_p^{\ell_2}$ is removed. Specifically, we discard shapelet $s_p^{\ell_2}$ if:

$$\text{Sim}(s_k^{\ell_1}, s_p^{\ell_2}) < \tau_{\text{sim}} \quad (19)$$

where τ_{sim} is a threshold to determine whether two shapelets are too similar.

D. Shapelets Positioning

We usually use window to search similarity, but convolution offers several advantages over sliding windows for similarity calculation: It reduces computational overhead through optimized matrix operations, ideal for large datasets or long time series. It enables simultaneous similarity calculations, outperforming sequential sliding windows. It integrates well with GPU or hardware acceleration, making it effective for high-dimensional or multivariate time series.

After we extracted a set of representative shapelets s_1, s_2, \dots, s_n from the dataset, to find which MTS these shapelets correspond to, each shapelet is treated as a convolution kernel. Then we calculate the convolution similarity between shapelets and MTS. Let s be a shapelet with length L_s . The convolution operation is performed by sliding the shapelet over the time series T as (20). The convolution result $C(i)$ represents the similarity between the shapelet and the subsequence of the time series at position i .

$$C(i) = \sum_{j=0}^{L_s-1} T(i+j) \cdot s(j), \quad \text{for } i = 0, 1, \dots, L_t - L_s \quad (20)$$

A threshold ϵ is set to determine whether the similarity is significant as (21). If the convolution result at a certain position is less than ϵ , it indicates that the subsequence at position i is considered to be similar to the shapelet s .

$$\max C(i) > \epsilon \quad (21)$$

E. Subject information embedding

To prevent subject label information from interfering with weight updates, obtain subject features, and differentiate between each individual, we use the T5 [33] model to embed subject text label information. For example, the label can be "The patient is 20 years old" or "The patient has a certain disease", which will be embedded to feature vector. If the dataset does not have text information, we convert the subject label information into one-hot encoding to serve as subject features.

F. Heterogeneous Graph Constructing

In this study, we consider two additional types of information: **shapelets** and **subject differences**. As shown in the figure, we construct a heterogeneous graph containing MTS data. The set of nodes is $V = V_T \cup V_s \cup V_{\text{sub}}$. $T = \{T_1, \dots, T_m\}$ represents the MTS. $s = \{s_1, \dots, s_k\}$ represents the shapelets in the time series. $\text{sub} = \{\text{sub}_1, \dots, \text{sub}_n\}$ represents subject differences, such as different patients, age groups, or data

collection timestamps. The set of edges E represents the relationships between MTS T , shapelets s , and subject differences sub .

The steps of constructing the heterogeneous graph are as follows:

Shapelet: We have used a shapelet mining algorithm to extract significant local patterns s (III-C). These patterns are highly representative of certain categories. Then, for each MTS, we establish connections to the shapelets. If a MTS contains a particular shapelet, an edge is created between MTS and the corresponding shapelet. For each subject, if the shapelet comes from the corresponding subject, an edge is established. **Subject Differences:** To capture subject differences in the dataset III-E (e.g., different patients, age groups, or variations in data collection timestamps), we establish connections between each MTS and the relevant subject information. For instance, if a MTS is associated with a particular age group of patients or collected during a specific time period, an edge is created between that MTS and the corresponding subject node. In this way, we incorporate shapelet and subject differences into the heterogeneous graph representation.

After obtaining the above information, we consider the cross-relationship between them consisting of MTS, subjects, and shapelets. Based on these relationships, we built a heterogeneous graph, and the graph is symmetric, meaning the relationship between any two connected nodes is bidirectional or mutual. The heterogeneous graph \mathcal{A} is represented as Fig. 8, which is composed of various block matrices M , where N is the number of dimensions. The each parts of heterogeneous graph \mathcal{A} is detailed as follows:

MTS and MTS: Connected based on similarity (detailed in Section III-B2)). MTS and subject: Linked through corresponding relationships (e.g., a subject is associated with a specific MTS). MTS and shapelet: Connected through similarity, where a shapelet originates from a specific MTS (detailed in Section III-D). subject and subject: We do not create edges between them and set them to 0. subject and shapelet: Linked through corresponding relationships (e.g., shapelets belong to subjects). Shapelet and shapelet (computed using soft DTW loss as Section III-B2)): Connected based on similarity (e.g., similar patterns among shapelets). After obtaining the heterogeneous graph, we need to embed each type of information as node features, that is, MTS representation (detailed in Section III-B2)), subject features (detailed in Section III-E) and subject shapelets (detailed in Section III-C).

G. Heterogeneous Graph Representation Learning

We employ a dual level GAT to learn representations for heterogeneous graphs, consisting of type-level and node-level attention mechanisms. This mechanism enhances heterogeneous GAT by focusing on significant types and nodes, capturing richer relational structures.

The normalized adjacency matrix is $\tilde{\mathcal{A}} = M^{-1/2} \mathcal{A} M^{-1/2}$. The node representations in layer l are denoted as $G^{(l)} \in \mathbb{R}^{|V| \times q}$, with $G^{(0)} = F_{\text{node}}$. A heterogeneous graph with node

types are as MTS T_{rep} , subjects F_{sub} , and shapelets s . Let $\mathcal{C} = \{\kappa_1, \kappa_2, \kappa_3\}$ represent these types.

Then, the heterogeneous GAT is initially defined as 22. Initially, $G_{\kappa}^{(0)} = X_{\kappa}$.

$$G^{(k+1)} = \sigma \left(\sum_{\kappa \in \mathcal{C}} \tilde{\mathcal{A}}_{\kappa} \cdot G_{\kappa}^{(k)} \cdot M_{\kappa}^{(k)} \right), \quad (22)$$

where $\tilde{\mathcal{A}}_{\kappa} \in \mathbb{R}^{|V| \times |V_{\kappa}|}$ selects neighbors of type κ , $G_{\kappa}^{(k)}$ is the feature matrix for type κ at layer k , and $M_{\kappa}^{(k)} \in \mathbb{R}^{p^{(k)} \times p^{(k+1)}}$ projects type-specific features into a shared space.

In heterogeneous GAT, each node's influence depends on its neighbors' types. Nodes from the same type tend to provide more relevant information, but their importance varies. To capture these nuances, a dual-level attention includes type-level and node-level attention.

Type-level Attention: For a node v , type-level attention assesses the significance of neighboring nodes from different type. The embedding for each type κ is computed as (23).

$$a_{\kappa} = \sigma \left(\left\langle \xi_{\kappa}, \left[g_v; \sum_{v' \in \mathbf{N}_v, \text{type}(v')=\kappa} g_{v'} \right] \right\rangle \right), \quad (23)$$

where g_v and $g_{v'}$ are embeddings for node v and its neighbor v' of type κ . ξ_{κ} is a learnable attention vector for κ , $\sigma(\cdot)$ is an activation. $(;)$ denotes concatenation. Then, we use softmax to normalize these scores as $\alpha_{\kappa} = \exp(a_{\kappa}) / (\sum_{\kappa' \in \mathcal{C}} \exp(a_{\kappa'}))^{-1}$, where α_{κ} is the attention weight for type κ .

Node-level Attention: Node-level attention focuses on the influence of subject neighbors. Given a node v (type κ) and its neighbor v' (type κ'), we compute node-level attention as (24), where η is a learnable vector. We normalize $b_{vv'}$ across all neighbors as $\beta_{vv'} = \exp(b_{vv'}) / (\sum_{j \in \mathbf{N}_v} \exp(b_{vj}))^{-1}$.

$$b_{vv'} = \sigma(\langle \eta, \alpha_{\kappa'} \cdot [g_v; g_{v'}] \rangle), \quad (24)$$

Dual-level Graph Attention: Finally, combining both attention levels, the layer-wise propagation for node embeddings is computed as (25).

$$G^{(k+1)} = \sigma \left(\sum_{\kappa \in \mathcal{C}} \mathcal{B}_{\kappa} \cdot G_{\kappa}^{(k)} \cdot M_{\kappa}^{(k)} \right), \quad (25)$$

where \mathcal{B}_{κ} is an attention matrix with $\beta_{vv'}$ as entries, $G_{\kappa}^{(k)}$ is the feature matrix for category κ at layer k , and $M_{\kappa}^{(k)}$ is a learnable transformation matrix.

We finish node classification by softmax as:

$$\hat{Y} = \text{softmax}(W \cdot G^{(K)}) \quad (26)$$

where \hat{Y} is the predicted class labels for each node in the graph after applying the softmax function. W is the weight matrix that transforms the final node embeddings for classification.

IV. EXPERIMENTS

A. Experimental Setup

1) *Dataset:* We conducted classification studies on 12 public MTS datasets, including HAR [34] and sleep stage classification (ISRUC-3) [35], and 10 datasets from the UEA archive [36]: AF (Atrial Fibrillation), FM (Finger Movements), HMD (Hand Movement Direction), HB (Heartbeat), LIB (Libras), MI (Motor Imagery), NATO (NATOPS), PD (PenDigits), SRS2 (Self Regulation SCP2), and SWJ (Stand Walk Jump). These datasets represent the common intersection used by various comparative methods in existing study, ensuring the comparability and validity of our research. For HAR and ISRUC-3 datasets, we randomly split them into 80% for training and 20% for testing, while the UEA datasets followed their predefined train-test splits. And We used 10% of the labeled data.

The details of the dataset are as follows.

1) HAR: This dataset contains sensor data from 30 subjects performing six daily activities (walking, upstairs, downstairs, standing, sitting, lying). Data were collected using a Samsung Galaxy S2 device worn on the subject's waist, with a sampling rate of 50 Hz. The training set contains 7352 samples, the test set contains 2947 samples, the time series length is 128, the number of channels is 9, and there are 6 activity classes. The participants' ages range from 19 to 48 years.

2) ISRUC-3: This dataset contains 8589 samples from 10 healthy subjects aged 30 to 58. The data includes 2 electrooculography channels, 2 electromyography channels, 1 electrocardiogram channel, and 6 electroencephalogram channels in each polysomnography recording, all sampled at 200 Hz. The dataset is with 6871 in the training set and 1718 in the test set, used to evaluate model performance on different physiological signals.

3) The UEA MTS Classification Archive includes 10 datasets used for MTS classification experiments. The main features and statistics of each dataset are summarized in Table. I.

TABLE I: 10 datasets description.

Abbre	Train	Test	Dimension	Length	Classes
AF	15	15	2	640	3
FM	316	100	28	50	2
HMD	160	74	10	400	4
HB	204	205	61	405	2
LIB	180	180	2	45	15
MI	278	100	64	3000	2
NATO	180	180	24	51	6
PD	7494	3498	2	8	10
SRS2	200	180	7	1152	2
SWJ	12	15	4	2500	3

2) *Comparison Methods:* For UEA: we compared 15 implementations of the following MTS classifiers, covering traditional methods, deep learning methods, and GNN based methods. These methods are respectively: ED, DTWI, DTWD [36], WEASEL+MUSE [37], HIVE-COTE [38], MLSTM-FCN [39], TapNet [40], MTPool [41], MF-Net [42], Smate

[43], USRL [5], ShapeNet [44], Dyformer [45], TodyNet [12], MICOS [46], SVP-T [10], DKN [47].

For HAR & ISRUC-3: we compare our method with state-of-the-art methods, including SimCLR [48], TNC [49], TS-TCC [8], TS2Vec [50], MHCCL [51], CaSS [52], TAGCN [53], CA-TCC [7], TS-GAC [23].

3) *Experimental Environment*: All models were trained in a Python 3.8 environment using PyTorch 1.10.0 with Cuda 11.3, with training lasting for 1000 epochs. The training environment was configured with the Ubuntu 20.04 operating system, equipped with an NVIDIA GeForce RTX 2080 GPU (20GB VRAM) and an Intel(R) Xeon(R) Platinum 8352V CPU (48GB RAM).

4) *Experimental Parameters*: The initial learning rate was initially set to 10^{-3} , and we used Negative Log Likelihood Loss as the loss function to optimize the model parameters. Additionally, the Adam optimizer with ReduceLROnPlateau strategy was employed for parameter updates. For datasets without clear subject labels, we set the labels of all subject categories to 1, indicating that there is no subjects information. When calculating self-attention, the overlap ratio γ_1 is set to 0.5. When selecting anchor T_{to}^{ref} , we randomly select $m = \frac{C}{3}$ dimensions from C dimensions.

B. Experimental Analysis

Table II presents the accuracy of HGRL compared to 19 other MTS methods across 10 UEA datasets. Table III compares the performance of HGRL with 17 other methods on the HAR and ISRUC-3 datasets. In the results, the best performances are highlighted in bold, with "AVG" indicating the average accuracy of the method across all datasets, and "Wins" representing the number of times the method achieved the best accuracy on different datasets.

According to Table II, HGRL outperformed other advanced MTS classification methods on 4 datasets, achieving the highest average accuracy of 0.717. It demonstrated remarkable adaptability and competitiveness when handling datasets with varying numbers of variables and sequence lengths. The ranking of Critical Difference (CD) Fig. 4 further illustrates HGRL's overall performance across all datasets, where HGRL ranked first, providing strong evidence for the superiority of this method.

As shown in Table III, our method also achieved the best accuracy on the HAR (0.942) and ISRUC-3 (0.844) datasets, further validating the advantages of HGRL in MTS classification tasks. The superior results of our method can be attributed primarily to its robust information integration capabilities and flexible representation learning approach. Firstly, HGRL enhances classification performance by integrating various information (such as shapelets, subject features, and MTS representations) to fully exploit the potential value of different types of data. Secondly, the introduction of a dual attention mechanism (node-level and type-level) not only identifies the importance of samples but also clarifies the relationships between different types of information, enhancing the model's

understanding of MTS information and making classification more reliable.

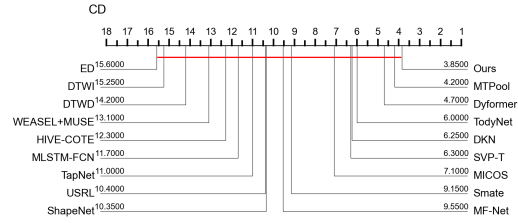


Fig. 4: UEA CD diagram.

C. HGRL's variants

According to the analysis of the results in Table IV and Fig. 5, when GCN is used instead of GAT for validation, HGRL (GCN) generally performs poorly across different datasets, indicating that GCN overlooks the heterogeneity of diverse information and struggles to capture complex time series features. On the FM, HMD, and HB datasets, GCN's performance is inferior to other methods.

The introduction of a type-level attention in HGRL (Type) improves performance on most datasets compared to GCN-HGRL, but it still falls short of the node-level attention in HGRL (Node). For example, on the HB dataset, HGRL (Node) achieves an accuracy of 0.678, higher than HGRL (Type)'s 0.663, indicating that node-level attention is more critical for time series classification. Ultimately, HGRL, which combines both type-level and node-level attention, performs best across all datasets, particularly achieving the highest accuracy of 0.889 on the LIB dataset, validating the complementarity and effectiveness of the double graph attention.

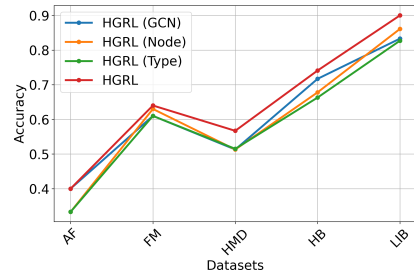


Fig. 5: Accuracy of HGRL's variants

D. Ablation Study

We validate the contributions of various Modules in the HGRL model through module ablation experiments. Specifically, we tested classification using the CTSA module (the random dimensions and principal dimensions), learned sub-shapelets (the single-scale and multi-scale shapelets), and the HGRL model with cross-entropy loss for classification. The results in Table V and Fig. 6 demonstrate that the full HGRL model yields the best performance. For example, on the AF dataset, HGRL achieves an accuracy of 0.4, while

TABLE II: Accuracy of Various Methods on the UEA Datasets

	AF	FM	HMD	HB	LIB	MI	NATO	PD	SRS2	SWJ	AVG	Wins
ED	0.267	0.519	0.279	0.620	0.833	0.510	0.850	0.973	0.483	0.333	0.567	0
DTWI	0.267	0.513	0.297	0.659	0.894	0.390	0.850	0.939	0.533	0.200	0.554	0
DTWD	0.267	0.529	0.231	0.717	0.872	0.500	0.883	0.977	0.539	0.200	0.572	0
WEASEL+MUSE	0.400	0.550	0.365	0.727	0.894	0.500	0.870	0.948	0.460	0.267	0.598	0
HIVE-COTE	0.133	0.550	0.446	0.722	0.900	0.610	0.889	0.934	0.461	0.333	0.598	0
MLSTM-FCN	0.333	0.580	0.527	0.663	0.850	0.510	0.900	0.978	0.472	0.400	0.621	0
TapNet	0.200	0.470	0.338	0.751	0.878	0.590	0.939	0.980	0.550	0.133	0.583	0
MTPool	0.533	0.620	0.486	0.742	0.900	0.630	0.944	0.983	0.600	0.667	0.711	1
MF-Net	0.466	0.620	0.445	0.692	0.850	0.540	0.927	0.983	0.533	0.400	0.646	0
Smate	0.133	0.620	0.554	0.741	0.849	0.590	0.922	0.980	0.567	0.533	0.649	0
USRL	0.333	0.530	0.378	0.751	0.850	0.590	0.939	0.980	0.550	0.400	0.630	0
ShapeNet	0.400	0.580	0.338	0.338	0.856	0.610	0.883	0.977	0.578	0.533	0.609	0
DKN	0.467	0.600	0.662	0.765	0.900	0.620	0.872	0.948	0.600	0.533	0.697	1
TodyNet	0.467	0.570	0.649	0.756	0.850	0.640	0.972	0.987	0.550	0.467	0.691	1
SVP-T	0.400	0.600	0.392	0.790	0.883	0.650	0.906	0.983	0.600	0.467	0.667	0
MICOS	0.333	0.570	0.649	0.766	0.889	0.500	0.967	0.981	0.578	0.533	0.677	0
Dyformer	0.267	0.650	0.459	0.816	0.944	0.640	0.933	0.997	0.628	0.433	0.677	4
Ours	0.400	0.640	0.567	0.741	0.900	0.660	0.972	0.980	0.644	0.667	0.717	4

TABLE III: Accuracy on the HAR and ISRUC-3 Datasets

	HAR	ISRUC-S3
SimCLR	0.899	0.750
TNC	0.811	0.776
TS-TCC	0.916	0.805
TS2Vec	0.927	0.763
MHCCL	0.829	0.747
CaSS	0.826	0.810
TAGCN	0.928	0.772
TS-GAC	0.942	0.842
CA-TCC	0.883	Null
Ours	0.942	0.844

TABLE IV: Accuracy of HGRL’s variants

	HGRL (GCN)	HGRL (Node)	HGRL (Type)	HGRL
AF	0.400	0.333	0.333	0.400
FM	0.610	0.630	0.610	0.640
HMD	0.513	0.513	0.515	0.567
HB	0.717	0.678	0.663	0.741
LIB	0.833	0.861	0.827	0.900

using the CTSA with random dimensions or subshapelets results in an accuracy of 0.333. However, when using the CTSA with principal dimensions, the accuracy improves to 0.4, highlighting the importance of principal dimensions.

Additionally, the performance of the MTS representation surpasses that of subshapelets, indicating that MTS representation plays a more crucial role in classification tasks. Overall, the synergistic effect of each module significantly enhances the model’s performance.

TABLE V: Accuracy of various Modules

	Only CTSA (random)	Only CTSA (principal)	Only subshapelets	Only subshapelets HGRL (multi-scale)	HGRL
AF	0.333	0.400	0.333	0.333	0.400
FM	0.600	0.610	0.530	0.540	0.640
HMD	0.554	0.554	0.283	0.337	0.567
HB	0.717	0.721	0.663	0.673	0.741
LIB	0.856	0.844	0.833	0.850	0.900

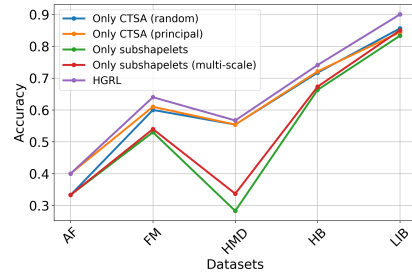


Fig. 6: Accuracy of various Modules

E. Analysis of the number of shapelets

According to the analysis of Table VI and Fig. 7, the accuracy of the HAR dataset increases from 0.924 to 0.931 as the number of shapelets increases from 32 to 128, indicating that performance improves with the increasing quantity. However, when the number of shapelets rises to 256 and 512, the accuracy slightly decreases, suggesting potential overfitting or information redundancy.

The results in the table indicate that different datasets have varying sensitivities to the number of shapelets. For example, the HAR and LIB datasets perform best with 128 shapelets, while HMD shows better results with 64 shapelets. An excessive number of shapelets may lead to overfitting or information redundancy: in all three datasets, the accuracy decreased after exceeding a certain number of shapelets, indicating that the number of shapelets should not be increased indefinitely.

TABLE VI: Accuracy of different number of shapelets

	HAR	HMD	LIB
32	0.924	0.500	0.833
64	0.932	0.567	0.883
128	0.943	0.527	0.890
256	0.931	0.527	0.888
512	0.931	0.500	0.893

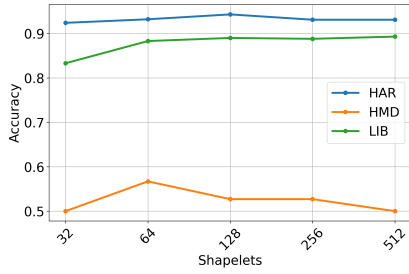


Fig. 7: Accuracy of different number of shapelets

F. Case study

As shown in Fig. 8, we choose the AF dataset to analyze the heterogeneous graph construction process. As shown in Fig. 8, it contains three types of information: MTS ($N_T = 30$), subjects ($N_{sub} = 2$), and shapelets ($N_s = 12$). Each small block matrix represents the relationship between them. And the matrix is symmetric. $M_{T,T}$ indicates the similarity between MTSs, and the diagonal line is the highest similarity. $M_{T,sub}$ indicates which subject each MTS belongs to. $M_{T,s}$ indicates the correspondence between MTSs and shapelets through the most similar search. $M_{sub,sub}$ indicates there is no clear relationship between subject and subject, and the diagonal line indicates a self-loop. $M_{sub,s}$ finds the correspondence by finding the individual MTSs corresponding to the shapelets. $M_{s,s}$ indicates the similarity between shapelets.

This analysis highlights the complex interrelationships within the dataset, highlighting the importance of each type of information in building a comprehensive heterogeneous graph. By studying these relationships, we can better understand the structure and dynamics of the dataset, which is crucial for enhancing representation learning and improving performance on subsequent tasks.



Fig. 8: Heterogeneous graph of AF dataset

V. CONCLUSION

In this study, we represent MTS datasets as heterogeneous graphs, incorporating both subject-specific features and

shapelet information for enhanced MTS node classification. And, we introduce a contrast temporal self-attention method for MTS representation learning, utilizing soft DTW to effectively capture similarities between MTS representations. At the same time, our method is designed to be interpretable, with learned shapelets that reflect subject-specific differences.

Looking ahead, we aim to explore more effective representation methods for MTS and heterogeneous graph representation methods. Additionally, we will develop effective aggregation methods for node information within heterogeneous graphs to better utilize various types of information and enhance classification performance.

VI. ACKNOWLEDGMENT

This work was supported by the National Natural Science Foundation of China [grant numbers 82072014], the National Key R&D Program of China [grant numbers 2019YFE010670], the Shandong Province Natural Science Foundation [grant numbers ZR2020MF028]. We would like to thank Eamonn Keogh and his team, Tony Bagnall and his team for the UEA/UCR time series classification repository.

REFERENCES

- [1] M. M. Rahman, M. A. Farahani, and T. Wuest, "Multivariate time-series classification of critical events from industrial drying hopper operations: A deep learning approach," *Journal of Manufacturing and Materials Processing*, 2023. DOI: 10.3390/jmmp7050164
- [2] L. Sun, M. Zhang, B. Wang, and P. Tiwari, "Few-shot class-incremental learning for medical time series classification," *IEEE J. Biomed. Health Inform.*, vol. PP, pp. 1872–1882, Feb. 22 2023.
- [3] D. Cheng, F. Yang, S. Xiang, and J. Liu, "Financial time series forecasting with multi-modality graph neural network," *Pattern Recognit.*, vol. 121, p. 108218, 2022. DOI: 10.1016/j.patrec.2021.108218
- [4] M. A. A. Al-qaness, A. Dahou, M. E. A. Elaziz, and A. M. Helmi, "Multi-resatt: Multilevel residual network with attention for human activity recognition using wearable sensors," *IEEE Trans. Industr. Inform.*, vol. 19, no. 1, pp. 144–152, 2023. DOI: 10.1109/TII.2022.3165875
- [5] J.-Y. Franceschi, A. Dieuleveut, and M. Jaggi, *Unsupervised scalable representation learning for multivariate time series*. Red Hook, NY, USA: Curran Associates Inc., 2019.
- [6] Z. Liang, J. Zhang, C. Liang, H. Wang, Z. Liang, and L. Pan, "A shapelet-based framework for unsupervised multivariate time series representation learning," *Proc. VLDB Endow.*, vol. 17, no. 3, p. 386–399, Nov. 2023. [Online]. Available: <https://doi.org/DOI:10.14778/3632093.3632103>
- [7] E. Eldele, M. Ragab, Z. Chen, M. Wu, C. Kwok, X. Li, and C. Guan, "Self-supervised contrastive representation learning for semi-supervised time-series classification," *IEEE Transactions on Pattern Analysis and Machine Intelligence*, vol. 45, pp. 15 604–15 618, 2022.
- [8] E. Eldele, M. Ragab, Z. Chen, M. Wu, C. K. Kwok, X. Li, et al., "Time-series representation learning via temporal and contextual contrasting," in *Proceedings of the Thirtieth International Joint Conference on Artificial Intelligence, IJCAI-21*, Z.-H. Zhou, Ed. International Joint Conferences on Artificial Intelligence Organization, 8 2021, pp. 2352–2359, main Track. [Online]. Available: <https://doi.org/DOI:10.24963/ijcai.2021/324>
- [9] G. Zerveas, S. Jayaraman, D. Patel, A. Bhamidipaty, and C. Eickhoff, "A transformer-based framework for multivariate time series representation learning," *Proceedings of the 27th ACM SIGKDD Conference on Knowledge Discovery & Data Mining*, 2020.
- [10] R. Zuo, G. Li, B. Choi, S. S. Bhowmick, D. N.-y. Mah, and G. L. Wong, "Svp-t: A shape-level variable-position transformer for multivariate time series classification," *Proceedings of the AAAI Conference on Artificial Intelligence*, vol. 37, no. 9, pp. 11 497–11 505, Jun. 2023. [Online]. Available: <https://ojs.aaai.org/index.php/AAAI/article/view/26359> DOI: 10.1609/aaai.v37i9.26359

- [11] M. Jin, H. Y. Koh, Q. Wen, D. Zambon, C. Alippi, G. I. Webb, et al., “A survey on graph neural networks for time series: Forecasting, classification, imputation, and anomaly detection,” *IEEE transactions on pattern analysis and machine intelligence*, vol. PP, 2023.
- [12] H. Liu, D. Yang, X. Liu, X. Chen, Z. Liang, H. Wang, et al., “Todynnet: Temporal dynamic graph neural network for multivariate time series classification,” *Inf. Sci.*, vol. 677, p. 120914, 2024. DOI: 10.1016/j.ins.2024.120914
- [13] Y. Wang, Z. Duan, Y. Huang, H. Xu, J. Feng, and A. Ren, “Mthetgnn: A heterogeneous graph embedding framework for multivariate time series forecasting,” *Pattern Recognit. Lett.*, vol. 153, pp. 151–158, 2022. DOI: 10.1016/j.patrec.2021.12.008
- [14] S. Xiang, D. Cheng, C. Shang, Y. Zhang, and Y. Liang, “Temporal and heterogeneous graph neural network for financial time series prediction,” *Proceedings of the 31st ACM International Conference on Information & Knowledge Management*, 2022. DOI: 10.1145/3511808.3557089
- [15] Z. Jia, Y. Lin, Y. Zhou, X. Cai, P. Zheng, Q. Li, et al., “Exploiting interactivity and heterogeneity for sleep stage classification via heterogeneous graph neural network,” *ICASSP 2023 - 2023 IEEE International Conference on Acoustics, Speech and Signal Processing (ICASSP)*, pp. 1–5, 2023. DOI: 10.1109/ICASSP49357.2023.10095397
- [16] Y. Wang, Z. Duan, B. Liao, F. Wu, and Y. Zhuang, “Heterogeneous attributed network embedding with graph convolutional networks,” in *AAAI Conference on Artificial Intelligence*, 2019. DOI: 10.1609/aaai.v33i01.330110061
- [17] T. Yang, L. Hu, C. Shi, H. Ji, X. Li, and L. Nie, “Hgat: Heterogeneous graph attention networks for semi-supervised short text classification,” *ACM Trans. Inf. Syst.*, vol. 39, no. 3, pp. 1–29, 2021. (TOIS) DOI: 10.1145/3450352
- [18] L. Ye and E. Keogh, “Time series shapelets: a new primitive for data mining,” in *Proceedings of the 15th ACM SIGKDD International Conference on Knowledge Discovery and Data Mining, ser. KDD '09*. New York, NY, USA: Association for Computing Machinery, 2009, p. 947–956. DOI: 10.1145/1557019.1557122
- [19] X.-M. T. Le, M.-T. Tran, and V.-N. Huynh, “Learning perceptual position-aware shapelets for time series classification,” in *ECML/PKDD*, 2022.
- [20] J. Grabocka, N. Schilling, M. Wistuba, and L. Schmidt-Thieme, “Learning time-series shapelets,” *Proceedings of the 20th ACM SIGKDD international conference on Knowledge discovery and data mining*, 2014. DOI: 10.1145/2623330.2623613
- [21] Q. Ma, W. Zhuang, and G. Cottrell, “Triple-shapelet networks for time series classification,” *2019 IEEE International Conference on Data Mining (ICDM)*, pp. 1246–1251, 2019. DOI: 10.1109/ICDM.2019.00155
- [22] Z. Cheng, Y. Yang, S. Jiang, W. Hu, Z. Ying, Z. Chai, et al., “Time2graph+: Bridging time series and graph representation learning via multiple attentions,” *IEEE Trans. Knowl. Data Eng.*, vol. 35, no. 2, pp. 2078–2090, 2023.
- [23] Y. Wang, Y. Xu, J. Yang, M. Wu, X. Li, L. Xie, et al., “Graph-aware contrasting for multivariate time-series classification,” in *Proceedings of the AAAI Conference on Artificial Intelligence*, vol. 38, no. 14, 2024, pp. 15 725–15 734.
- [24] T. Kipf and M. Welling, “Semi-supervised classification with graph convolutional networks,” *ArXiv*, vol. abs/1609.02907, 2016.
- [25] D. Zha, K.-H. Lai, K. Zhou, and X. Hu, “Towards similarity-aware time-series classification,” in *Proceedings of the 2022 SIAM International Conference on Data Mining (SDM)*. SIAM, 2022, pp. 199–207. DOI: 10.1137/1.9781611977172.23
- [26] W. Xi, A. Jain, L. Zhang, and J. Lin, “Efficient and accurate similarity-aware graph neural network for semi-supervised time series classification,” in *Pacific-Asia Conference on Knowledge Discovery and Data Mining*. Springer, 2024, pp. 276–287. DOI: 10.1007/978-981-97-2266-2_22
- [27] S. Mao and X.-J. Zeng, “Learning visibility attention graph representation for time series forecasting,” *Proceedings of the 32nd ACM International Conference on Information and Knowledge Management*, 2023. DOI: 10.1145/3583780.3615289
- [28] Z. Liu, Q. Ma, P. Ma, and L. Wang, “Temporal-frequency co-training for time series semi-supervised learning,” in *AAAI Conference on Artificial Intelligence*, 2023. DOI: 10.1609/aaai.v37i7.26072
- [29] L. Zhang and B. J. Mortazavi, “Semi-supervised meta-learning for multi-source heterogeneity in time-series data,” in *Machine Learning in Health Care*, 2023.
- [30] Z. Liu, W. Pei, D. Lan, and Q. Ma, “Diffusion language-shapelets for semi-supervised time-series classification,” in *AAAI Conference on Artificial Intelligence*, 2024. DOI: 10.5772/intechopen.111293
- [31] F. Schroff, D. Kalenichenko, and J. Philbin, “Facenet: A unified embedding for face recognition and clustering,” *2015 IEEE Conference on Computer Vision and Pattern Recognition (CVPR)*, pp. 815–823, 2015. DOI: 10.1109/CVPR.2015.7298682
- [32] M. Cuturi and M. Blondel, “Soft-dtw: a differentiable loss function for time-series,” in *International Conference on Machine Learning*, 2017.
- [33] J. Ni, G. Hernandez Abrego, N. Constant, J. Ma, K. Hall, D. Cer, et al., “Sentence-15: Scalable sentence encoders from pre-trained text-to-text models,” in *Findings of the Association for Computational Linguistics: ACL*, S. Muresan, P. Nakov, and A. Villavicencio, Eds. Dublin, Ireland: Association for Computational Linguistics, May, 2022, pp. 1864–1874.
- [34] D. Anguita, A. Ghio, L. Oneto, X. Parra, and J. L. Reyes-Ortiz, “A public domain dataset for human activity recognition using smartphones,” in *The European Symposium on Artificial Neural Networks*, 2013.
- [35] S. Khalighi, T. Sousa, J. M. Santos, and U. Nunes, “ISRUC-Sleep: A comprehensive public dataset for sleep researchers,” *Comput. Methods Programs Biomed.*, vol. 124, pp. 180–192, Feb. 2016. DOI: 10.1016/j.cmpb.2015.10.013
- [36] A. Bagnall, H. A. Dau, J. Lines, M. Flynn, J. Large, A. Bostrom, et al., “The uea multivariate time series classification archive, 2018,” *arXiv preprint arXiv*, 2018.
- [37] P. Schäfer and U. Leser, “Multivariate time series classification with weasel+ muse,” *arXiv preprint arXiv*, 2017.
- [38] A. Bagnall, M. Flynn, J. Large, J. Lines, and M. Middlehurst, “A tale of two toolkits, report the third: on the usage and performance of hivedcote v1. 0,” *arXiv preprint arXiv*, 2020.
- [39] F. Karim, S. Majumdar, H. Darabi, and S. Harford, “Multivariate LSTM-FCNs for time series classification,” *Neural Netw.*, vol. 116, pp. 237–245, Aug. 2019. DOI: 10.1016/j.neunet.2019.04.014
- [40] X. Zhang, Y. Gao, J. Lin, and C.-T. Lu, “Tapnet: Multivariate time series classification with attentional prototypical network,” *Proc. Conf. AAAI Artif. Intell.*, vol. 34, no. 04, pp. 6845–6852, 2020. DOI: 10.1609/aaai.v34i04.6165
- [41] Z. Duan, H. Xu, Y. Wang, Y. Huang, A. Ren, Z. Xu, et al., “Multivariate time-series classification with hierarchical variational graph pooling,” *Neural Netw.*, vol. 154, pp. 481–490, Oct. 2022. DOI: 10.1016/j.neunet.2022.07.032
- [42] M. Du, Y. Wei, X. Zheng, and C. Ji, “Multi-feature based network for multivariate time series classification,” *Inf. Sci.*, vol. 639, p. 119009, 2023. DOI: 10.1016/j.ins.2023.119009
- [43] J. Zuo, K. Zeitouni, and Y. Taher, “Smate: Semi-supervised spatio-temporal representation learning on multivariate time series,” in *2021 IEEE International Conference on Data Mining (ICDM)*. IEEE, 2021, pp. 1565–1570. DOI: 10.1109/ICDM51629.2021.00206
- [44] G. Li, B. Choi, J. Xu, S. S. Bhowmick, K.-P. Chun, and G. L.-H. Wong, “Shapenet: A shapelet-neural network approach for multivariate time series classification,” *Proc. Conf. AAAI Artif. Intell.*, vol. 35, no. 9, pp. 8375–8383, May 2021. DOI: 10.1609/aaai.v35i9.17018
- [45] C. Yang, X. Wang, L. Yao, G. Long, and G. Xu, “Dyformer: A dynamic transformer-based architecture for multivariate time series classification,” *Inf. Sci.*, vol. 656, p. 119881, 2024. DOI: 10.1016/j.ins.2023.119881
- [46] S. Hao, Z. Wang, A. D. Alexander, J. Yuan, and W. Zhang, “Micos: Mixed supervised contrastive learning for multivariate time series classification,” *Knowl. Base. Syst.*, vol. 260, p. 110158, 2023. DOI: 10.1016/j.knosys.2022.110158
- [47] Z. Xiao, H. Xing, R. Qu, L. Feng, S. Luo, P. Dai, et al., “Densely knowledge-aware network for multivariate time series classification,” *IEEE Trans. Syst. Man Cybern. Syst.*, vol. 54, no. 4, pp. 2192–2204, 2024. DOI: 10.1109/TSMC.2023.3342640
- [48] T. Chen, S. Kornblith, M. Norouzi, and G. Hinton, “A simple framework for contrastive learning of visual representations,” ser. *ICML'20*. JMLR.org, 2020.
- [49] S. Tonekaboni, D. Eytan, and A. Goldenberg, “Unsupervised representation learning for time series with temporal neighborhood coding,” *ArXiv*, vol. abs/2106.00750, 2021.

- [50] Z. Yue, Y. Wang, J. Duan, T. Yang, C. Huang, Y. Tong, et al., "Ts2vec: Towards universal representation of time series," in *AAAI Conference on Artificial Intelligence*, 2021.
- [51] Q. Meng, H. Qian, Y. Liu, Y. Xu, Z. Shen, and L. zhen Cui, "Mhccl: Masked hierarchical cluster-wise contrastive learning for multivariate time series," in *AAAI Conference on Artificial Intelligence*, 2022.
- [52] Y. Chen, X. Zhou, Z. Xing, Z. Liu, and M. Xu, "Cass: A channel-aware self-supervised representation learning framework for multivariate time series classification," in *International Conference on Database Systems for Advanced Applications*, 2022. DOI: 10.1007/978-3-031-00126-0_29
- [53] X. Zhang, Y. Wang, L. Zhang, B. Jin, and H. Zhang, "Exploring unsupervised multivariate time series representation learning for chronic disease diagnosis," *Int. J. Data Sci. Anal.*, vol. 15, no. 2, pp. 173–186, 2023. DOI: 10.1007/s41060-021-00290-0